

## SURFACE-ENHANCED RAMAN SCATTERING-BASED IMMUNOASSAY OF TWO CYTOKINES IN HUMAN GINGIVAL CREVICULAR FLUID OF PERIODONTAL DISEASE

H. Yang<sup>1</sup>, M. L. Zhang<sup>2</sup>, L. H. Yao<sup>3</sup>, M. Zhou<sup>4</sup>,  
Q. Wang<sup>5</sup>, Yu Chen<sup>5</sup>, Y. Ding<sup>5\*</sup>

<sup>1</sup> Chengdu First People's Hospital, Chengdu, 610041, China

<sup>2</sup> Chongqing Share dent Clinic, Chongqing, 400010, China

<sup>3</sup> The First Affiliated Hospital of Zhengzhou University, Henan, 450000, China

<sup>4</sup> Stomatological Hospital of Chongqing Medical University, Chongqing, 400017, China

<sup>5</sup> State Key Laboratory of Oral Diseases, National Clinical Research Center for Oral Diseases, West China Hospital of Stomatology, Sichuan University, Chengdu, 610041, China;  
e-mail: jessie.yh@163.com, hengyang2911@qq.com

*This study combined Raman technology and nanotechnology to detect periodontal inflammatory factors. We synthesized silver nanoparticles and made modifications to their surface to produce Ag NP-antibody probes. A sandwich immunoassay was developed for the sensitive detection of TNF- $\alpha$  and IL-1 $\beta$ . SERS intensity showed a good linear relationship with TNF- $\alpha$  and IL-1 $\beta$  concentrations in our study. The results of detection of these biomarkers in GCF indicate excellent specificity, high sensitivity, and great reproducibility of this immunoassay. Our immunoassay based on the SERS technique would facilitate clinical diagnoses of periodontal diseases.*

**Keywords:** periodontal disease, gingival crevicular fluid, surface-enhanced Raman scattering, cytokines, inflammation.

## ИММУНОАНАЛИЗ ДВУХ ЦИТОКИНОВ В ДЕСНЕВОЙ ЖИДКОСТИ ЧЕЛОВЕКА ПРИ ЗАБОЛЕВАНИЯХ ПАРОДОНТА НА ОСНОВЕ СПЕКТРОСКОПИИ ПОВЕРХНОСТНО-УСИЛЕННОГО КОМБИНАЦИОННОГО РАССЕЯНИЯ

H. Yang<sup>1</sup>, M. L. Zhang<sup>2</sup>, L. H. Yao<sup>3</sup>, M. Zhou<sup>4</sup>,  
Q. Wang<sup>5</sup>, Yu Chen<sup>5</sup>, Y. Ding<sup>5\*</sup>

УДК 535.375.5;616.314.17-008.1

<sup>1</sup> Первая народная больница Чэнду, Чэнду, 610041, Китай

<sup>2</sup> Чунцинская стоматологическая клиника, Чунцин, 400010, Китай

<sup>3</sup> Первая больница университета Чжэнчжоу, Хэнань, 450000, Китай

<sup>4</sup> Стоматологическая больница Чунцинского медицинского университета, Чунцин, 400017, Китай

<sup>5</sup> Национальный центр клинических исследований заболеваний полости рта, Западно-Китайская стоматологическая больница, Университет Сычуань, Чэнду, 610041, Китай; e-mail: jessie.yh@163.com, hengyang2911@qq.com

(Поступила 8 октября 2018)

*Исследована возможность совместного использования гигантского комбинационного рассеяния (ГКР) и нанотехнологии для определения факторов воспаления пародонта. Для создания маркеров антител синтезированы наночастицы серебра и осуществлена модификация их поверхности. Разработан метод поэтапного иммуноанализа для чувствительного детектирования цитокинов ФНО- $\alpha$  и Ил-1 $\beta$ . Получена линейная зависимость интенсивности ГКР от концентрации цитокинов ФНО- $\alpha$  и Ил-1 $\beta$ . Результаты детектирования этих биомаркеров в десневой кревicularной жидко-*

сти показали, что разработанный метод обладает высокой степенью избирательности и хорошей воспроизводимостью иммуноанализа.

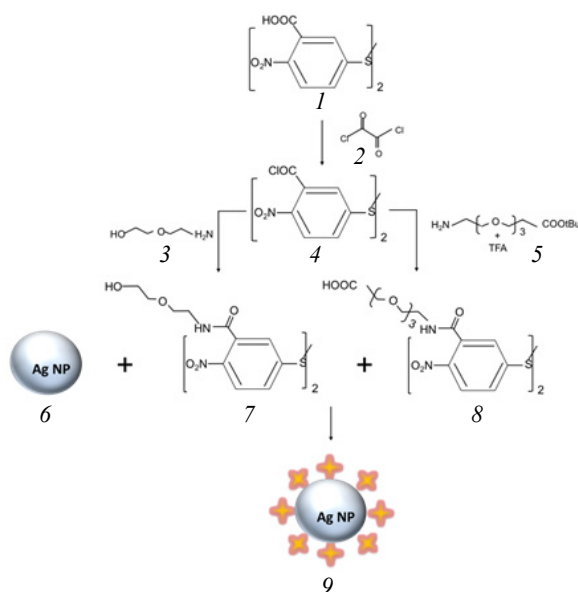
**Ключевые слова:** пародонтит, десневая кревicularная жидкость, гигантское комбинационное рассеяние, цитокины, воспаление.

**Introduction.** Periodontitis is a chronic inflammatory disease, in which inflammatory cytokines and tissue-destructive molecules are overproduced in response to microbial pathogens [1]. These cytokines and molecules travel from the inflamed tissues to the gingival crevicular fluid (GCF), then enter the saliva and accumulate there, and can potentially serve as biomarkers for periodontal diseases [2–7]. However, the currently available diagnostic methods for periodontitis, including clinical tests and radiological approaches, are insufficient to make an objective and accurate diagnosis. As there are higher levels of various enzymes and mediators in GCF of patients with periodontal diseases than in healthy individuals, these biomolecules in GCF have served as a diagnostic target for early detection of periodontitis and a risk factor of progression, as well as to monitor the responses to periodontal treatments [8, 9].

Surface-enhanced Raman scattering (SERS) is a recently-emerging technique that can be used to selectively detect biomolecules such as peptides, proteins, and nucleic acids [10–15]. The SERS method has several advantages including reduced susceptibility to photo-bleaching, narrow width of vibrational Raman bands at spectral multiplexing, and high sensitivity. SERS immunoassays are potentially an alternative to enzyme-linked immunosorbent assays (ELISAs), but are somewhat superior in that they can detect and even quantify multiple targets in a mixture in one single SERS measurement. Therefore, in this assay a small amount, of samples is needed, the overall cost is reduced, but a higher efficiency is provided [16–19].

In this study, Ag-nanoparticles (Ag-NPs) were synthesized and modified with hydrophilically-stabilized molecules. Then they were used as SERS labels in a sandwich immunoassay that detected inflammatory cytokines on functionalized glass slides, in combination with microspectroscopic detection with a high spatial resolution.

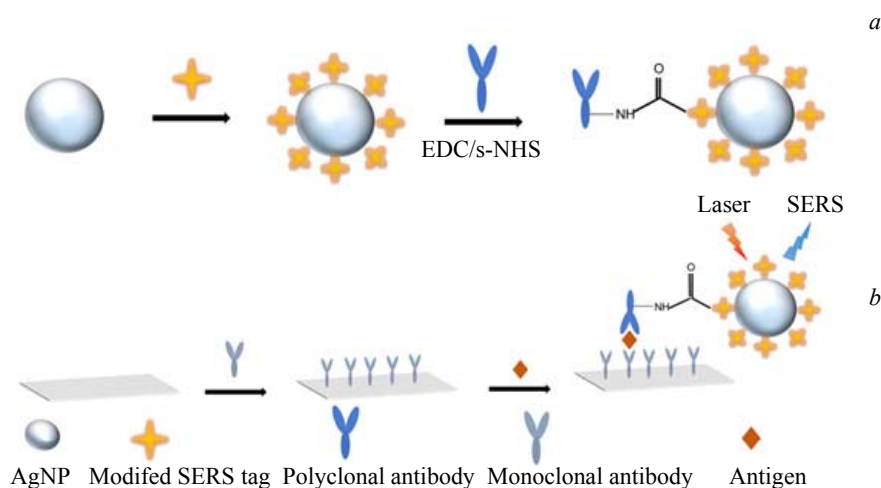
**Experimental.** Silver nitrate ( $\text{AgNO}_3$ ), sodium citrate, 4-mercaptobenzoic acid (4MBA), 5,5'-dithio-bis(2-nitrobenzoic acid) (DTNB), aminoethoxyethanol, trifluoroacetic acid (TFA), N-(3-dimethylaminopropyl)-N'-ethyl-carbodiimide (EDC), N-hydroxysulfosuccinimide sodium salt (s-NHS), tert-butyl-3-[2-(2-(2-aminoethoxy)ethoxy)ethoxy]ethonal, tris-(tris(hydroxymethyl)aminomethane), 4-(2-hydroxyethyl)-1-piperazineethanesulfonic acid (HEPES), bovine serum albumin (BSA),  $\text{NaHCO}_3$ , sodium chloride (NaCl),  $\text{Na}_2\text{HPO}_4$ ,  $\text{KH}_2\text{PO}_4$ , sodium acetate hydrate, ethanol, anhydrous ethylene glycol, and polyvinylpyrrolidone (PVP) were purchased from Sigma/Aldrich/Fluka. Monoclonal anti-human TNF- $\alpha$ (MAB610), IL-1 $\beta$ (MAB601) antibody, human TNF- $\alpha$ (AF-210-NA), IL-1 $\beta$ (AF-201-NA) affinity purified polyclonal antibody, and recombinant human TNF- $\alpha$ (210-TA-005/CF), IL-1 $\beta$  (201-LB-005/CF) were purchased from R&D systems Inc.



Scheme 1. Preparation and modification of Ag-NPs.

Silver colloids were prepared according to the method reported by Lee et al. [20]. Briefly, an aqueous 2 mL solution containing 0.1 M  $\text{AgNO}_3$  and 0.15 M PVP was added into 194 mL boiling water under vigorous stirring. Then 4 mL 1% sodium citrate solution was added and the whole kept boiling for ~60 min. The mixture solution was cooled down to room temperature (RT) with stirring and centrifuged at 1920 g for 15 min (Thermo LEGEND Micro 17R, USA) to precipitate the silver colloids, which were then redispersed in double-distilled  $\text{H}_2\text{O}$  and stored at  $4^\circ\text{C}$  in the dark until use. The maximum of absorption was determined to be at 420 nm by UV-Vis-spectroscopy (HITACHI, Japan), suggesting a diameter of ~40–60 nm. DTNB and 4-MBA were used as Raman reporter signals to qualitatively and quantitatively analyze IL-1 $\beta$  and TNF- $\alpha$ . They were modified by a short spacer unit monoethylene glycol (-MEG-OH) and a longer spacer unit triethylene glycol (-TEG-COOH) according to Jehn's study [21].

The above separated 1 mL silver colloidal solution containing Ag-NPs was dissolved in 1 mL solution containing 1 mM of modified Raman-active reporter units (stoichiometric ratio of DTNB-MEG-OH to DTNB-TEG-COOH 100:1, and 4MBA-MEG-OH to 4MBA-TEG-COOH 100:1). After a 15-min ultrasonic bath, a 4-h stirring was applied. After formation of a complete self-assembled monolayer (SAM), the colloid was washed twice with  $\text{H}_2\text{O}$  double distilled and centrifuged for 15 min at 1920 g, then redispersed in 500  $\mu\text{L}$  HEPES. The colloidal solution was activated by EDC/s-NHS for 30 min under shaking and centrifuged at 1920 g for 15 min. The supernatant containing excess EDC/s-NHS was removed, and the colloid was redispersed in 500  $\mu\text{L}$  HEPES buffer (pH 5.9). Polyclonal anti-IL-1 $\beta$  or -TNF- $\alpha$  (0.5  $\mu\text{g}$ ) antibody was then added to the 500  $\mu\text{L}$  colloid suspension which contained activated SERS label (DTNB or 4MBA) and reacted at RT for 1 h followed by standing at  $4^\circ\text{C}$  overnight to produce the antibody-SERS label conjugates. Then 400  $\mu\text{L}$  of Tris-Tween 20 buffer containing 0.2% BSA was added to 500  $\mu\text{L}$  suspension of antibody-SERS label conjugate and incubated at RT for 15 min with shaking to minimize nonspecific binding by blocking the particle surface. After that, the SERS-labeled antibodies were washed three times with Tris-Tween 20 buffer containing 0.2% BSA and centrifuged at 1920 g for 15 min at  $4^\circ\text{C}$ . The precipitate of SERS-labeled antibodies was redispersed in 500  $\mu\text{L}$  of Tris-Tween 20 buffer containing 0.2% BSA and used to bind the functionalized glass surface.



Scheme 2. Ag NPs modified with SERS tag and labeled with antibody (a); SERS immunoassay of IL-1 $\beta$  and TNF- $\alpha$  (b)

*Preparation of immune substrates.* Monoclonal antibody of IL-1 $\beta$  or TNF- $\alpha$  was bound on Polymer 3-digital glass slides (JingXin<sup>®</sup>, Capitalbio Corporation, Shanghai, China). The glass surface was divided into three parts, and each was incubated with 2  $\mu\text{g}/\text{mL}$  monoclonal antibody in 30  $\mu\text{L}$  carbonate buffer I (CBI) (0.2 M  $\text{NaHCO}_3$ , 0.5 M  $\text{NaCl}$ ; pH 8.5) at RT for 1 h followed by standing at  $4^\circ\text{C}$  overnight. The glass slides were washed three times (with shaking) with carbonate buffer II (CBII) (containing 0.1 M  $\text{NaHCO}_3$  and 0.5 M  $\text{NaCl}$ , pH 8.0) followed by acetate buffer (0.1 M sodium acetate, pH 4.4) and PBST buffer (PBS with 0.05% Tween 20, pH 7.4) (once for each). After that, they were blocked with 2% BSA for 2 h at RT to minimize nonspecific binding, washed three times with PBST, and dried under a nitrogen atmosphere. Then they were incubated with human recombinant IL-1 $\beta$  (hrIL-1 $\beta$ ) or human recombinant TNF- $\alpha$  (hrTNF- $\alpha$ )

(10, 1, and 100  $\mu\text{g/mL}$ ; 10, 1  $\text{ng/mL}$ ; 100, 10, 1  $\text{pg/mL}$ ) or 2% BSA as a negative control at RT for 1 h followed by 4°C overnight.

*Separate detection of IL-1 $\beta$  and TNF- $\alpha$ .* IL-1 $\beta$  was detected with DTNB-labeled Ag-NPs with anti-TNF- $\alpha$ , while TNF- $\alpha$  was detected with 4MBA-labeled Ag-NPs with anti-IL-1 $\beta$ . The glass slides prepared as above were washed three times again with PBST and then incubated with SERS-labeled antibodies at RT for 1 h followed by standing at 4°C overnight. Typically, 10  $\mu\text{L}$  of the prepared SERS probes were pipetted onto the substrate at the exact positions where IL-1 $\beta$  or TNF- $\alpha$  were previously located, with the concentrations of SERS labels at each addition being normalized to the optical density of the colloid to ensure reproducibility. Afterwards, the glass slides were washed with PBST three times and dried under a nitrogen atmosphere before measurement.

*SERS-based immunoassay of TNF- $\alpha$  and IL-1 $\beta$  in human GCF.* Ten patients clinically diagnosed with gingivitis (G group), 10 patients with chronic periodontitis (P group), and 10 healthy individuals (C group) participated in this study. The criteria for inclusion in the G and P groups were based on Carranza's Clinical Periodontology, 11th Edition. Pregnant women and individuals with systemic disease were excluded. All participants received oral examinations to exclude obvious oral lesions; they were not taking hyposalivation-inducing drugs or other prescription or non-prescription drugs. The study was approved by the Ethics Committee of West China Hospital of Stomatology, Sichuan University [No. WCHSIRB-OT-2013-055].

GCF was collected from all the participants [22]. Briefly, after slightly removing plaques and calculus around a tooth and drying the area, a Periopaper strip was placed directly into the gingival sulcus or a periodontal pocket for 60 s. The volume of collected GCF was quantified on a Periotron (Harco, Tustin, CA), and the paper strip was placed in 1 mL of normal saline solution in a 1.5 mL micropipette tube. The samples were immediately shaken for 1 h, then centrifuged at 6000 g for 15 min at 4°C. The supernatant was stored at 20°C until use in the assays.

**Instrumentation and statistical analysis.** A Raman microspectrometer (LabRam, Horiba-Jobin-Yvon) equipped with a microscope, a monochromator with a grating of 950 grooves per millimeter, and a Peltier-cooled CCD camera were used to perform the Raman experiments. With a 50 $\times$  microscope objective (Olympus, model LM Plan Fl, NA D 0.5) with a power of 1 mW, radiation from the 632.8 nm line of a He-Ne laser was focused on the sample. The SERS spectrum was analyzed by Labspec 5 and Origin 9 software. The data were expressed as mean  $\pm$  SEM and analyzed with one-way analysis of variance (ANOVA) using a SPSS software (SPSS 17.0, Chicago, IL);  $p < 0.05$  was considered to be statistically significant.

**Results and discussion.** *Characterization of Ag-NPs and antibody-SERS label conjugates.* Ag-NPs were generated from a chemical reduction reaction between AgNO<sub>3</sub> and sodium citrate, according to a previously reported procedure by Lee and co-workers [20]. The synthesized silver colloids had a maximum absorption at  $\sim$ 420 nm, suggesting that they had a diameter of  $\sim$ 40–60 nm. PVP is a good stabilizer [23], which produces silver nanowires with a high aspect ratio and SERS activity, so it was employed in this study to avoid silver colloid aggregation. The SERS labels consist of gold nanoparticles (Au-NPs) coated with a SAM of arylthiols and can be used as Raman reporter molecules as introduced by Porter and co-workers [24]. The use of SAM ensures that a maximum amount of Raman label molecules would be covered on the metal surface, co-adsorption of other molecules from the environment to the metal surface would be minimized, and molecules have a uniform orientation relative to the surface, which benefits uniform enhancement of Raman signals.

In this study, the Raman reporters were modified by covalent conjugation of MEG-OH and TEG-COOH, to the nitro aromatic disulfide of DTNB and 4-MBA. The use of MEG-OH and TEG-COOH provides benefits of increasing the stability of the SERS labels due to the EG (ethylene glycol) termini and making bio-conjugation controllable via the MEG-OH/TEG-COOH stoichiometry [22]. A stoichiometric MEG-OH/TEG-COOH ratio of 100:1 was adopted to provide steric accessibility of the carboxyl groups in the densely packed SAM [25]. With the addition of DTNB-/4MBA-MEG-OH and DTNB-/4MBA-TEG-COOH, the metal colloid formed a self-assembled monolayer with hydrophilic stabilization, which was comprised of two different terminal spacer units. The Raman reporter molecules were packed closely and densely within the SAM on Ag-NPs, thus preventing as much as possible the co-adsorption of other molecules from the environment onto the surface of Ag-NPs. Then EDC/s-NHS was added to activate the carboxyl groups in the SAM to form bio-conjugate to the antibodies.

In this study, pegylation of Raman reporter units DTNB and 4MBA did not influence the SERS spectrum (Fig. 1). In addition, the SERS label in this study produced very similar Raman spectrum as those by NHS-activated (curve 1) and antibody-conjugated (curve 3) SERS labels (Fig. 1). These results suggest that

the functionalization of SERS labels DTNB-MEG/-TEG and 4-MBA-MEG/-TEG does not have a significant impact on the label signature.

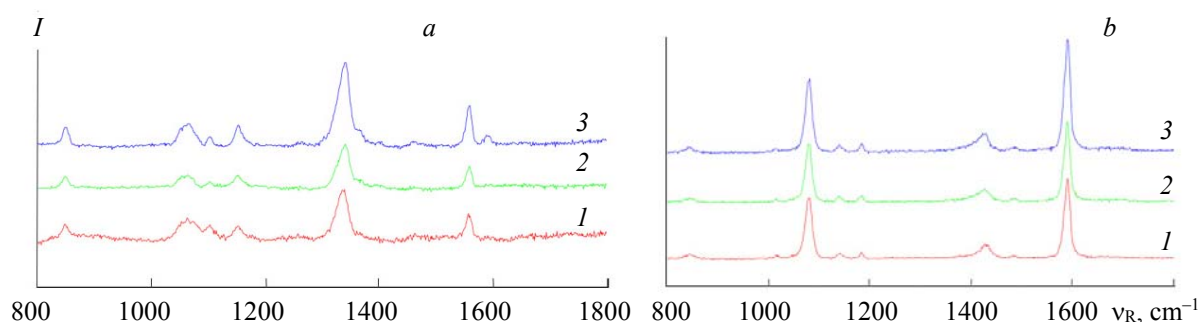


Fig. 1. SERS spectra of SERS substrate SAM of DTNB-MEG/TEG (a) and SAM of 4MBA-MEG/TEG (b) modified by Raman reporter molecule before (1) and after activated by EDC/s-NHS (2) and antibodies (3).

*Reproducibility and sensitivity of hrTNF- $\alpha$  and hrIL-1 $\beta$  SERS immunoassay.* In the SERS immunoassay, DTNB and 4MBA were used as labels for Ag-NPs bound by poly-antibodies for IL-1 $\beta$  (probe A) or TNF- $\alpha$  (probe B). After adding a solution of hrIL-1 $\beta$  or hrTNF- $\alpha$ , the mono-antibodies for hrIL-1 $\beta$  and hrTNF- $\alpha$  were added and captured on the glass slides. Following the immune-capture reaction, the mono-antibody, antigens, as well as DTNB- and 4MBA-labeled antibody formed a sandwich-like conjugate on the glass slide.

To evaluate the specificity of this immunoassay, probe A was tested in the presence of both hrIL-1 $\beta$  and hrTNF- $\alpha$  at the same concentration of 1  $\mu\text{g/mL}$ . The SERS spectra (Fig. 2a) showed that the SERS intensity for hrIL-1 $\beta$  was much higher than that for hrTNF- $\alpha$  (nonspecific), indicating that probe A specifically recognizes hrIL-1 $\beta$ . Similarly, the specificity of probe B for hrTNF- $\alpha$  was demonstrated (Fig. 2b).

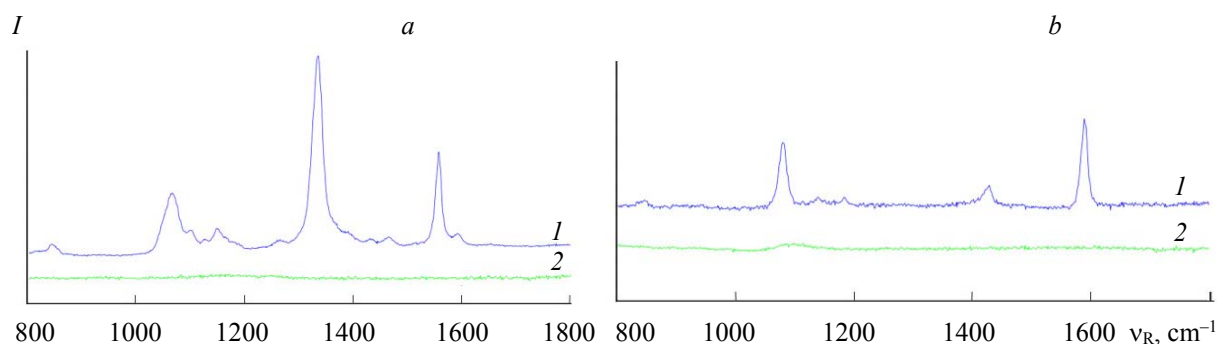


Fig. 2. SERS spectra of probe A exposed to IL-1 $\beta$  (1) and TNF- $\alpha$  (2) (a); SERS spectra of probe B exposed to IL-1 $\beta$  (nonspecific); and TNF- $\alpha$  (specific) (b); 1 — IL-1 $\beta$ , 2 — TNF- $\alpha$

To test for the sensitivity, solutions of hrTNF- $\alpha$  and hrIL-1 $\beta$  with series concentrations of 10  $\mu\text{g/mL}$ , 1  $\mu\text{g/mL}$ , 100  $\mu\text{g/mL}$ , 10  $\text{ng/mL}$ , 1  $\text{ng/mL}$ , 100  $\text{pg/mL}$ , 10  $\text{pg/mL}$ , and 1  $\text{pg/mL}$  were exposed to probe A, with 2% BSA used as a control. The SERS spectra corresponding to different concentrations of hrIL-1 $\beta$  and hrTNF- $\alpha$  exhibited a declining trend with decreasing concentrations (Fig. 3a). For hrIL-1 $\beta$ , the peak intensity at 1335  $\text{cm}^{-1}$  was used to characterize the SERS spectra. Figure 3b showed a nearly linear relationship between SERS intensity and hrIL-1 $\beta$  concentration, with calibration equation  $y = 8774.8 \log C + 126666$  and a correlation coefficient  $R^2 = 0.98236$  ( $n = 8$ ). The detection limit of hrIL-1 $\beta$  was  $\sim 10$   $\text{pg/mL}$ , suggesting that the SERS-based immunoassay in this study performed better than other ELISA methods with respect to sensitivity.

For hrTNF- $\alpha$  detection, the capability of probe B to detect a series of concentrations of hrTNF- $\alpha$  was tested by characterizing the SERS peak intensity at 1590  $\text{cm}^{-1}$ . Again, the SERS intensity well correlated with the concentration of hrTNF- $\alpha$  in a linear pattern, and the detection limit was as low as 10  $\text{pg/mL}$  (Fig. 3c,d). The calibration equation was  $y = 8112.2\log C + 116075$  with a correlation coefficient  $R^2 = 0.98582$  ( $n = 8$ ). These results demonstrated the highly increased sensitivity of immunoassays based on modified Ag-NPs, which were used for subsequent multiplex detection.

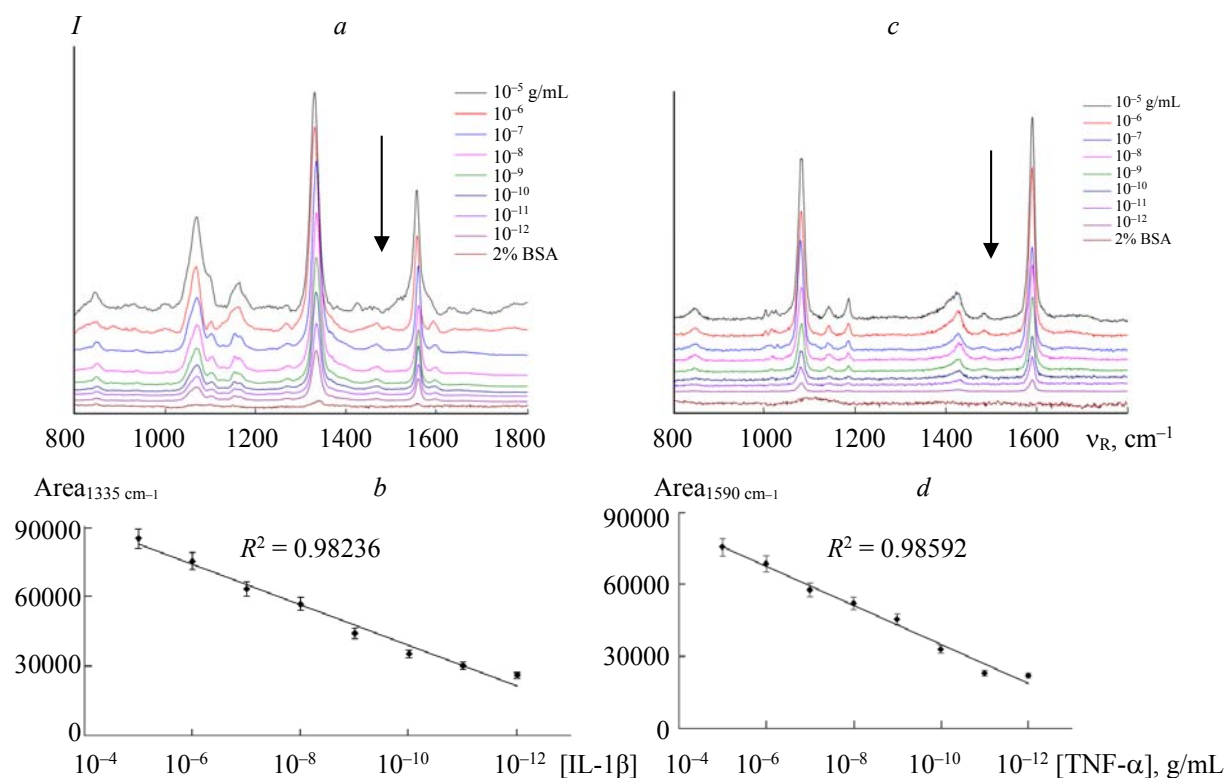


Fig. 3. (a) Concentration dependent SERS signal response for hrIL-1 $\beta$  detection, concentration ranges from  $10^{-5}$  to  $10^{-12}$  g/mL and with 2% BSA as blank control; (b) peak intensity at 1335  $\text{cm}^{-1}$  as a function of the hrIL-1 $\beta$  concentration. Calibration equation is  $y = 8774.8\log C + 126666$  with a correlation coefficient ( $R^2 = 0.98236$ ,  $n = 8$ ); (c) concentration dependent SERS signal response for hrTNF- $\alpha$  detection, concentration ranges from  $10^{-5}$  to  $10^{-12}$  g/mL and with 2% BSA as blank control; (d) peak intensity at 1590  $\text{cm}^{-1}$  as a function of the hrIL-1 $\beta$  concentration. Calibration equation is  $y = 8112.2\log C + 116075$  with a correlation coefficient ( $R^2 = 0.98582$ ,  $n = 8$ ).

*SERS-based quantitative immunoassay of TNF- $\alpha$  and IL-1 $\beta$  in human GCF.* The changes of inflammatory cytokines in human GCF reflect the transformation of periodontal disease, such as chronic periodontitis and gingivitis. The GCF could be the first test target to indicate host susceptibility to periodontal diseases. According to Gamonal's research [9], GCF volume collected from periodontitis patients by periostrips is up to 0.11–1.54  $\mu\text{L}$ , and 0.11–0.48  $\mu\text{L}$  in healthy individuals. Given that the quantity of GCF collected from each tooth is limited, a testing method with both high sensitivity and specificity is needed. The SERS-based immunoassay in this study seems to meet the need, as the lowest detectable concentrations of hrTNF- $\alpha$  and hrIL-1 $\beta$  were 10  $\text{pg/mL}$ .

In the present study, GCF samples collected from each group were detected three times to obtain the SERS spectra. The peak intensity at 1335 and 1590  $\text{cm}^{-1}$  was used to characterize the SERS spectra for IL-1 $\beta$  and TNF- $\alpha$ , respectively. The result showed that the SERS intensities for IL-1 $\beta$  and TNF- $\alpha$  in GCF (Fig. 4a,b) of the P group ( $67388.8 \pm 6132.5$ ,  $66866.8 \pm 5862.9$ ) and the G group ( $31419.2 \pm 4846.9$ ,  $32999.4 \pm 4577.8$ ) were significantly higher than those in the C group ( $21174.4 \pm 6062.1$ ,  $18576.6 \pm 4286.6$ ) ( $P = 0.00$ ) (Fig. 4c,d), consistent with results from ELISA, further confirming the high sensitivity and specificity as well as the applicability of this method.



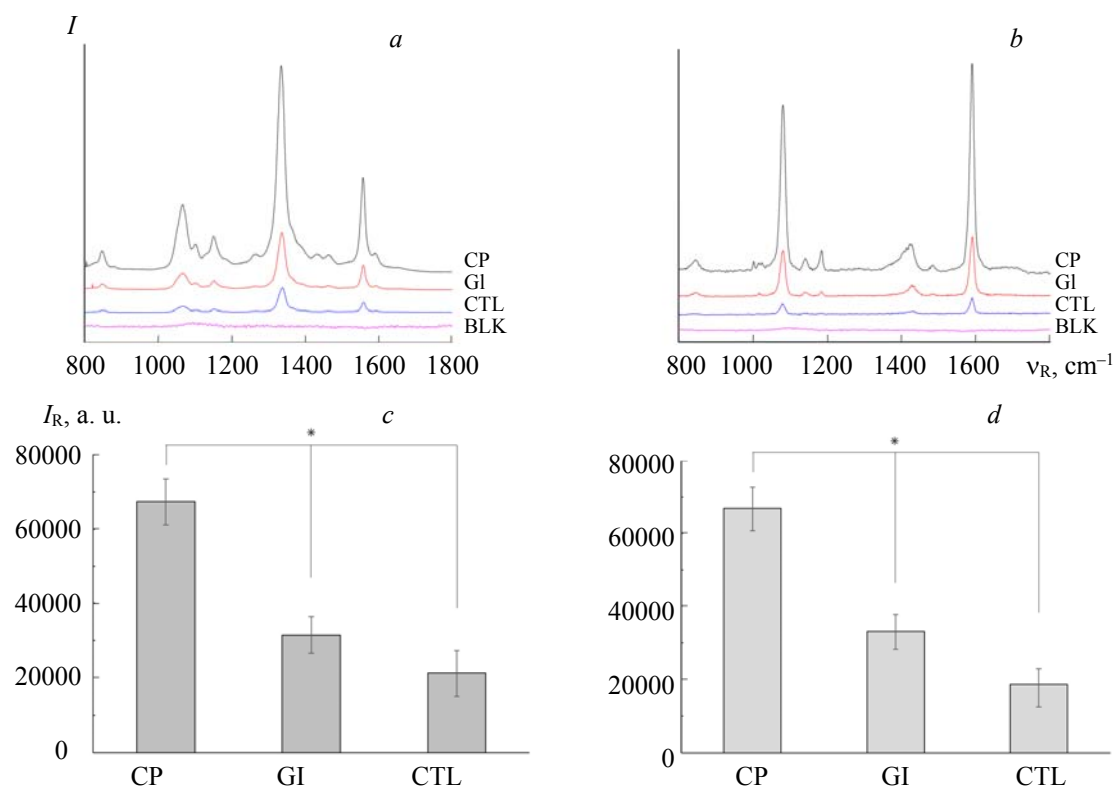


Fig. 4. Concentration dependent SERS spectra for IL-1 $\beta$ . (a) Detection using probe A and TNF- $\alpha$ ; (b) detection using probe B in GCF of different group. The peak intensity at 1335 and 1590  $\text{cm}^{-1}$  was used as a function of IL-1 $\beta$  (c) concentration and TNF- $\alpha$  (d) concentration; it showed a significant difference of SERS intensity of the P group (CP) compared to the G group (GI) and the C group (CTL) (CP is chronic periodontitis, GI is gingivitis, CTL is control).

**Conclusion.** As far as we know, this is the first report on the use of SERS-based immunoassay to detect the levels of TNF- $\alpha$  and IL-1 $\beta$  in human GCF with high sensitivity and specificity. Specifically, Ag-NPs were used as SERS label. The Raman reporters DTNB or 4MBA were conjugated with ethylene glycols with terminal groups -OH and -COOH and were arrayed as SAM on the Ag-NP surfaces. The hydrophilically stabilized dual-spacer SAM on Ag-NPs has a high stability, and the corresponding colloid will not precipitate. The lowest detectable concentrations for TNF- $\alpha$  and IL-1 $\beta$  are both 10  $\mu\text{g}/\text{mL}$  with modified Ag-NPs. As the SERS-based immunoassay here showed high sensitivity and specificity in detecting TNF- $\alpha$  and IL-1 $\beta$ , it is potentially clinically useful for clinical diagnostics in human samples, preferably with portable Raman instrumentation.

**Acknowledgment.** The work was performed with financial support from the National Key Basic Research and Development Program (grant No.2013CBA01700), National Nature Science Foundation of China (grant No. 81371149), and Chengdu Medical Research Project (No. 2018026).

## REFERENCES

1. B. L. Pihlstrom, B. S. Michalowicz, N. W. Johnson, *Lancet*, **366**, 1809–1820 (2005).
2. G. C. Armitage, *Periodontol.* **2000**, **34**, 109–119 (2004).
3. H. Ito, Y. Numabe, S. Hashimoto, S. Sekino, E. Murakashi, H. Ishiguro, *J. Periodontol.*, **87**, 1314–1319 (2016).
4. Q. Zhang, B. Chen, D. Zhu, F. Yan, *Arch. Oral. Biol.*, **72**, 92–98 (2016).
5. O. Cakmak, Z. Tasdemir, C. A. Aral, S. Dundar, H. B. Koca, *J. Clin. Periodontol.*, **43**, 1024–1031 (2016).
6. J. Liukkonen, U. K. Gürsoy, P. J. Pussinen, A. L. Suominen, E. Könönen, *J. Periodontol.*, **87**, 1484–1491 (2016).

7. M. Kuboniwa, A. Sakanaka, E. Hashino, T. Bamba, E. Fukusaki, A. Amano, *J. Dent. Res.*, **95**, 1381–1386 (2016).
8. R. C. Page, *J. Periodontol.*, **63**, 356–366 (1992).
9. J. Gamonal, A. Acevedo, A. Bascones, O. Jorge, *J. Periodontol.*, **71**, 1535–1545 (2000).
10. N. R. Isola, D. L. Stokes, T. Vo-Dinh, *Anal. Chem.*, **70**, 1352 (1998).
11. W. Ren, Y. Fang, E. Wang, *ACS Nano*, **5**, 6425–6433 (2011).
12. M. Y. Sha, H. Xu, M. J. Natan, R. Cromer, *J. Am. Chem. Soc.*, **130**, 17214–17215 (2008).
13. Y. C. Cao, R. Jin, C. A. Mirkin, *Science*, **297**, 1536 (2002).
14. Y. Chen, H. Cheng, K. Tram, S. Zhang, Y. Zhao, L. Han, Z. Chen, S. Huan, *Analyst*, **138**, 2624–26231 (2013).
15. L. Wu, Z. Wang, S. Zong, H. Chen, C. Wang, S. Xu, Y. Cui, *Analyst*, **138**, 3450–3456 (2013).
16. E. Papadopoulou, S. E. Bell, *Chemistry*, **18**, 5394 (2012).
17. G. F. Wang, R. J. Lipert, M. Jain, S. Kaur, S. Chakraborty, M. P. Torres, S. K. Batra, R. E. Brand, M. D. Porter, *Anal. Chem.*, **83**, 2554–2561 (2011).
18. H. Hwang, H. Chon, J. Choo, J. K. Park, *Anal. Chem.*, **82**, 7603–7610 (2010).
19. V. L. Schmit, R. Martoglio, K. T. Carron, *Anal. Chem.*, **84**, 4233–4236 (2012).
20. P. V. Lee, D. Meisel, *J. Phys. Chem.*, **86**, 3391–3395 (1982).
21. C. Jehn, B. Kustner, P. Adam, A. Marx, P. Strobel, C. Schmuck, S. Schlucker, *Phys. Chem. Chem. Phys.*, **11**, 7499–7504 (2009).
22. E. Papathanasiou, F. Teles, T. Griffin, E. Arguello, M. Finkelman, J. Hanley, *J. Periodont. Res.*, **49**, 55–61 (2014).
23. Y. G. Sun, Y. D. Yin, B. T. Mayers, T. Herricks, Y. N. Xia, *Chem. Mater.*, **14**, 4736–4745 (2002).
24. M. D. Porter, R. J. Lipert, L. M. Sioperko, G. Wang, R. Narayanan, *Chem. Soc. Rev.*, **37**, 1001–1011 (2008).
25. Y. Wang, M. Salehi, M. Schütz, K. Rudi, S. Schlucker, *Analyst*, **138**, 1764–1771 (2013).